



**HAL**  
open science

## Volume chirped Bragg gratings - monolithic components for stretching and compression of ultrashort laser pulses

L.B. Glebov, V. Smirnov, E. Rotari, I. Cohanoshi, L. N. Glebova, O. Smolski,  
J. Lumeau, C. Lantigua, A. Glebov

### ► To cite this version:

L.B. Glebov, V. Smirnov, E. Rotari, I. Cohanoshi, L. N. Glebova, et al.. Volume chirped Bragg gratings - monolithic components for stretching and compression of ultrashort laser pulses. *Optical Engineering*, 2014, 53 (5), pp.051514. hal-00945888

**HAL Id: hal-00945888**

**<https://hal.science/hal-00945888>**

Submitted on 13 Mar 2019

**HAL** is a multi-disciplinary open access archive for the deposit and dissemination of scientific research documents, whether they are published or not. The documents may come from teaching and research institutions in France or abroad, or from public or private research centers.

L'archive ouverte pluridisciplinaire **HAL**, est destinée au dépôt et à la diffusion de documents scientifiques de niveau recherche, publiés ou non, émanant des établissements d'enseignement et de recherche français ou étrangers, des laboratoires publics ou privés.

# **Volume chirped Bragg gratings – monolithic components for stretching and compression of ultrashort laser pulses**

Leonid Glebov<sup>1,2</sup>, Vadim Smirnov<sup>1</sup>, Eugeniu Rotari<sup>1</sup>, Ion Cohanoschi<sup>1</sup>, Larissa Glebova<sup>1</sup>, Oleg Smolski<sup>1</sup>, Julien Lumeau<sup>2</sup>, Christopher Lantigua<sup>2</sup>, Alexei Glebov<sup>1</sup>

<sup>1</sup> OptiGrate Corp. 562 S. Econ Circle, Oviedo, FL 32765

<sup>2</sup> University of Central Florida, CREOL/the College of Optics and Photonics. 4000 Central Florida Blvd. Orlando, FL 32816

## **Abstract**

A new type of optical component – a volume Bragg grating (VBG) – has recently become available commercially and has found wide applications in optics and photonics due to its unusually fine spectral and angular filtering capability. Reflecting volume Bragg gratings, with the grating period gradually changing along the beam propagation direction (chirped Bragg gratings, CBGs) provide stretching and recompression of ultra-short laser pulses. CBGs, being monolithic, are robust devices that have a footprint three orders of magnitude smaller than that of a conventional Treacy compressor. CBGs recorded in photo-thermo-refractive glass can be used in the spectral range from 0.8 to 2.5  $\mu\text{m}$  with the diffraction efficiency exceeding 90%, and provide stretching up to 1 ns and compression down to 200 fs for pulses with energies and average powers exceeding 1 mJ and 250 W, respectively, while keeping the recompressed beam quality  $M^2 < 1.4$ , and possibly as low as 1.1. This paper discusses fundamentals of stretching and

compression by CBGs, the main parameters of the gratings including the CBG effects on the laser beam quality, and currently achievable CBG specifications.

Key words: Chirped pulse amplification, chirped Bragg gratings, photo-thermo-refractive glass,

## **Introduction**

A number of applications of ultrashort laser pulses in medicine, industry and defense require high average power and high pulse energy. However, direct amplification of ultrashort pulses can induce detrimental nonlinear effects and/or laser-induced damage in amplifiers due to the extremely high peak power of the amplified pulses. A technique called chirped pulse amplification (CPA) was proposed in Ref. [1] to mitigate these effects. In this technique, low-power ultrashort pulses are stretched (“chirped”) in time and space using dispersive optical elements. Stretched pulses having lower power density are then amplified to a power level somewhat less than the damage-threshold of the amplifying system. The amplified chirped pulses are compressed by the same or similar dispersive optical elements that were used for stretching. The highest peak power that can be obtained using this technique is determined primarily by the optical damage threshold of the compressor components.

Initially, pulse stretching and compression in CPA systems was performed almost exclusively by pairs of surface diffraction gratings [2, 3] that usually are called “Treacy stretchers and compressors”. While the conventional technology that uses surface diffraction gratings provides a dramatic increase in the achievable power level, it has limitations associated with the reduced

average-power handling capacity of these components, which is typically in the range of tens of watts. With the availability today of fiber lasers operating at power levels easily exceeding 1 kW, this limitation has become the main obstacle to power-scaling of ultrashort pulse lasers.

Additionally, Treacy stretchers and compressors require highly-uniform, large-aperture gratings and large grating separation distances. Such stretchers and compressors are bulky, difficult to align, and susceptible to vibrations.

An important advancement in the development of CPA systems was made by the use of fiber-chirped Bragg gratings [4,5]. This approach has dramatically increased the robustness of CPA systems enabling their use in harsh environments outside of research laboratories. However, while fiber stretching became the conventional method for CPA systems design, the limited aperture of chirped fiber Bragg gratings imposes limitations on the peak power achievable with fiber-based pulse compressors due to nonlinear effects in the fibers and laser-induced damage of the fibers. To overcome these limitations, the use of volume chirped Bragg gratings for pulse stretching and compression has been proposed [6]. Initially, implementation of this proposal was slow to develop because of the absence of a suitable technology for fabrication of such optical elements. All of the photosensitive materials that were available at that time for volume hologram recording could not satisfy the requirements for high power applications in laser systems [7]. The situation changed when the bulk holographic material - photo-thermo-refractive (PTR) glass [8,9] - was developed [10] which further enabled the development of the technology of high efficiency volume Bragg gratings. The creation of volume chirped Bragg gratings (CBGs, volume Bragg gratings) with a variable period in the direction of the beam

propagation) recorded in PTR glass enabled a new approach to the design of high power stretchers and compressors, and has become an important, competing CPA technique [11-13].

A conventional compressor is based on a pair of surface diffraction gratings that must be placed at some distance from each other, and occupies a volume of several liters, not including the size of large aperture telescopes, mirrors, etc. A typical CBG enables decreasing the size and weight of compressors by several orders of magnitude – to 0.005 liter, for example. The most vulnerable feature of Treacy compressors is their high sensitivity to vibrations and shocks that result in misalignment between the diffraction gratings. The use of CBG stretchers and compressors enhances the robustness of CPA systems because these devices are monolithic, meaning there is nothing within the stretcher/compressor function to become misaligned (although it still must be aligned with the input beam). Thus these devices are inherently free from the effects of vibration and shocks. The main limitation of CBG stretchers and compressors at the current level of the technology of volume Bragg gratings recorded in PTR glass is a narrow spectral width that restricts operations to pulses longer than 100 fs.

### **Stretching and compression of laser pulses by volume CBGs**

A uniform volume Bragg grating is a phase volume hologram produced by recording the interference pattern of two collimated beams (Fig. 1A). This recording results in a spatial refractive index modulation (the creation of numerous planar layers having a modified refractive index) in the volume of the photosensitive optical material. These layers provide a resonant diffraction of optical beams that is described in [14] and detailed for engineering calculations in

[15, 16]. The diffraction of radiation inside of this grating occurs if the Bragg conditions are satisfied:

$$\theta_m = \frac{\lambda}{2nA}, \quad (1)$$

where  $\theta_m$  is the angle inside the photosensitive medium between a plane of constant refractive index and the direction of beam propagation,  $\lambda$  is the wavelength,  $n$  is the average refractive index, and  $A$  is the grating period. If a volume grating is positioned in such manner that the diffracted beam ( $\lambda_2$  in Fig. 2A) is deflected and crosses its back surface, this is defined as a transmitting Bragg grating. The beams that do not satisfy the Bragg conditions (either angle of incidence or wavelength or both) pass through the grating without changing their direction of propagation. If a volume grating is positioned in such a manner that the diffracted beam ( $\lambda_2$  in Fig. 2B) crosses the entrance surface, this is defined as a reflecting Bragg grating or a Bragg mirror. Bragg mirrors recorded in PTR glass with thicknesses from a fraction of a millimeter to several centimeters have spectral widths ranging from a few nanometers down to a few picometers. An example of a diffraction efficiency spectrum for a uniform reflecting grating is shown in Fig. 3 (curve 1). Like a transmitting grating, beams not meeting the Bragg conditions propagate through the reflecting grating without changing their direction of propagation.

While uniform volume gratings are recorded using an interference pattern produced by two collimated beams (Fig. 1A), it is possible to interfere a divergent beam with a convergent one (Fig. 1B). In this case the interference pattern consists of dark and bright planes with a period ( $A$ ) gradually changing in the Z direction perpendicular to a bisector of the recorded beams. If the

convergence and divergence angles are equal, the resulting volume reflecting Bragg grating would have a period linearly varying in the  $Z$  direction. If the period variation is directed along the beam propagation direction ( $Z$ ) of such an element, it is a longitudinal chirped reflecting volume Bragg grating depicted in Figs. 1B and 2C. A detailed model of beam propagation in CBGs is described in Ref. [17]. Thus, in this paper we will use a simplified description for the specification of the basic parameters of CBGs. It is clear that a CBG can be considered as the sum of a great number of uniform gratings with different periods which provide an increased spectral width compared to that of a uniform grating.

The reflection spectrum of a CBG depends on the chirp rate of the grating period,  $d\Lambda/dz$ . For normal incidence, Eq. (1) gives a resonant wavelength  $\lambda=2n\Lambda$ . Therefore a spectral chirp rate (SCR), which is the basic parameter of a CBG working close to the retroreflecting geometry, is determined as:

$$SCR = \frac{d\lambda}{dz} = 2n \frac{d\Lambda}{dz} \quad (2)$$

Such a grating can work as a wide band filter with a spectral width extending up to tens of nanometers depending on the SCR and the grating thickness as shown in Fig. 3 (curves 2 and 3).

The total spectral width of a CBG is the product of the SCR and its thickness ( $T$ ):

$$\Delta\lambda = SCR \times T \quad (3)$$

The capability of CBGs for stretching pulses is illustrated in Fig. 2C. One can see that different spectral components of a laser pulse would be reflected from different sections of the CBG. The total delay time (the maximum stretching),  $t_s$  between spectral components corresponding to the front and back ends of a CBG with not very high diffraction efficiency [17] is determined by:

$$t_s = \frac{2nT}{c}, \quad (4)$$

where  $n$  is an average refractive index of the CBG and  $c$  is the speed of light. This delay between spectral components of a laser pulse determines the ultimate time delay dispersion (TDD) or stretching factor (SF) of such a device:

$$SF = \frac{t_s}{\Delta\lambda} = \frac{2n}{c SCR} \quad (5)$$

This parameter (TDD or SF) is in common use for CPA system design with dimensionality [ps/nm]. For a given SCR, a simple way to estimate the SF for CBGs recorded in PTR glass with a refractive index close to  $n=1.5$  is:

$$SF, [ps/nm] = \frac{100}{SCR, [nm/cm]} \quad (6)$$

For an ideal CBG with a linear chirp, the delay of the different spectral components is a linear function of wavelength (a straight line in Fig. 4). In reality, the material dispersion of the photosensitive material, along with imperfections of a photosensitive material and within a hologram recording system, cause deviations from such a linear function. This distorted



dispersion curve is often modeled by polynomial functions where the linear term is equal to the stretching factor (Eq. 5) and higher order terms are called third order dispersion (TOD), etc.

Recording of phase volume Bragg gratings in PTR glass is a result of the refractive index change caused by photoinduced precipitation of sodium fluoride nanocrystals [18]. The refractive index modulation is proportional to the volume fraction of crystals precipitated in the volume of the PTR glass matrix [19]. While PTR glass is a highly transparent material, hologram recording causes some additional scattering and absorption [20]. This induced absorption is caused by silver and silver halides in the short wavelength spectral region ( $\lambda < 800$  nm) and by a valence change of different impurities in the longer wavelength range [21]. Induced scattering is the result of the precipitation of nanocrystals of sodium fluoride [18] and it is proportional to the concentration of those crystals [22]. The level of scattering in PTR glass containing a certain volume fraction of the crystalline phase is determined by the size of the crystals. The current technology results in a minimum size of crystals of about 15 nm; a further decrease of the crystal size would require the development of a new photosensitive material.

The spectral dependence of the scattering coefficient (the internal optical density divided by the thickness in centimeters)  $\alpha_s(\lambda)$  produced by particles with sizes far below visible or IR wavelengths is described by the Rayleigh formula:

$$\alpha_s(\lambda) = \alpha_{s0} \left( \frac{\lambda_0}{\lambda} \right)^4, \quad (7)$$

where  $\alpha_{s0}$  is the scattering coefficient at  $\lambda_0$ . These losses are small in the near IR spectral region – absorption is below  $10^{-3} \text{ cm}^{-1}$ , scattering is below  $10^{-2} \text{ cm}^{-1}$  and it dramatically decreases with wavelength increasing in accordance with formula (7). However, the thickness of CBGs that provide stretching for several hundred picoseconds is several centimeters. For stretching followed by compression, each spectral component propagates through a doubled thickness of the CBG. This means that for 5-cm-thick grating, the total attenuation in the vicinity of  $1 \text{ }\mu\text{m}$  could reach

$$A = 1 - 10^{-\alpha_s T} = 1 - 10^{-0.01 \times 10} \approx 0.2 \quad (8)$$

which would, therefore, significantly affect the properties of CBGs. For short wavelength compressors, the sharp dependence of scattering on wavelength results in high losses - losses exceeding 30% for 800 nm - yet results in almost lossless compressors in the vicinity of  $2 \text{ }\mu\text{m}$ . A decrease in the spectral width of CBGs (an increase in the stretching factor) will allow decreasing the required refractive index modulation, and those gratings will have lower losses as will be shown in the next Section.

An experimental diffraction spectrum of a CBG centered at 1555 nm is shown in Fig. 5 (curve 1). One can see that the absolute diffraction efficiency (a combination of relative diffraction efficiency and losses) at short wavelengths is lower than at longer wavelengths. It was confirmed that the relative diffraction efficiency, which is determined by the spatial refractive index modulation, is identical for all spectral components and the asymmetry in the diffraction spectrum is caused by losses. However, this asymmetry is not caused by the corresponding

asymmetry of absorption or scattering spectra (which are flat in this narrow spectral region) but is a result of illuminating the CBG from the end with the larger grating period (from the left side in Fig. 2C) which is called the “red end”. In this case, the spectral components with shorter wavelengths propagate longer distances and accumulate higher losses. Illumination of the same CBG from the “blue end” results in higher losses and a lower absolute diffraction efficiency for the long wavelength spectral components. Therefore, measurements of the different parameters of CBGs should refer to a direction of the exciting radiation from “red” or “blue” ends.

Sequential stretching and compression provides a symmetric spectrum because this CBG is sequentially illuminated from both ends.

It is important to note that the reflection spectrum of a CBG is close to a tabletop profile while the emission spectra of pulsed lasers are close to Gaussian in shape (Fig. 5). This means that for efficient reflection of the whole spectrum of a laser system, which is determined by the FWHM for a Gaussian function, a CBG should have about two times the spectral width of the FWHM for a tabletop function.

One can see from Eq. (4) that for stretching a laser pulse to 1 ns, a CBG with a thickness of 100 mm is necessary. This means that for stretching to this pulse length and further recompression of a laser pulse in the vicinity of 1  $\mu\text{m}$ , each spectral component propagates for 200 mm inside of a volume hologram recorded in PTR glass and crosses about 600,000 layers having a modified refractive index. This feature of the CBG technology necessitates strict requirements on the quality of the optical material (the optical homogeneity of PTR glass) and the quality of the holographic recording (the uniformity of the recorded interference pattern).

This is why one of the most important parameters of a CBG is the divergence of the stretched and compressed ultrashort pulse laser beams. The most commonly used laser beam quality metric is the  $M^2$  method accepted by the International Standardization Organization (ISO) [23]. The  $M^2$  factor of a beam is calculated by measuring the dependence of the beam radius on the distance from a plane where the beam is focused by an aberration-free lens and compared to this dependence for a diffraction-limited Gaussian beam.  $M^2$  is usually determined by the single diffraction of a beam with its spectral width adjusted to match the reflection spectrum of the CBG; this will be the metric for certification of CBGs.

However a number of applications based on threshold processes, e.g. ablation, require reliable data for the power density at the central spot of a laser beam on a target. This value has a good correlation with  $M^2$  if it is below 1.1. To provide reliable power density data for CBGs providing higher  $M^2$ , such a parameter as “power-in-the-bucket” [24, 25] is used. To enable a direct correlation of this parameter with  $M^2$  measured by means of commercial devices, a cylindrical “bucket” can be substituted having two orthogonal slits enabling an easy comparison of “power-in-the-bucket” with  $M^2$  in the corresponding directions.

As it was mentioned in Section 1, the main limitation in power scaling of ultrashort pulse lasers is the instantaneous peak power density that triggers a number of detrimental nonlinear effects. A CPA reduces this power density in an amplified laser pulse inversely with the stretching time and, therefore, enables a corresponding increase in pulse energy after amplification. This is why an increase in stretching time is usually considered as a promising method for peak power/ pulse energy scaling. Increasing the stretching time requires a proportional increase in the CBG

thickness (Eq. 4). This is limited by the current technology for fabricating large size PTR glass wafers and for recording large aperture holograms. However, it is possible to increase the stretching time (and further decrease power density) by providing multiple passes of the laser pulse through the CBG [26] or by designing multi-sectional devices consisting of several CBGs [27] (Fig. 6). The multiple pass geometry for stretching and compression is produced by the use of mirrors and beam steering optical components that provide an increase in the time delay between the different spectral components. One can see in Fig. 4 that a double pass through the same grating provides doubling of the stretching factor. Of course, this additional propagation length causes additional losses (about 8% in Fig. 5) but it enables a doubling of the stretching time and, therefore, almost double the pulse energy with the use of the same CPA device. It was shown in [27] that placing a sequence of several CBGs having adjacent reflection spectra and with proper spacing between them provides the same stretching and compression as a monolithic VBG with the same reflection spectrum and thickness. This approach enables the design of stretchers and compressors having an equivalent thickness that exceeds the current technological capability.

It should be noted that the use of multipass CBGs enables a new opportunity for pulse shape control [28]. One can see in Fig. 6A that after the first diffraction in the multipass geometry, different spectral components are dispersed in a direction perpendicular to the direction of the beam propagation. Placing a phase mask between a CBG and a mirror (Fig. 6A) provides a phase shift between the different spectral components. This shift results in pulse distortions in the time domain. An example from modeling is shown in Fig. 7. One can see that placing a binary phase mask that provides a phase shift of  $\lambda/2$  for half of the beam (this means half of the pulse

spectrum) causes a dramatic deformation in the pulse shape. It was found that the use of different phase masks could enable complex transformations in the pulse shape. Similarly, fine tuning of the spacing between sections of a multi-sectional compressor (Fig. 6B) provides a temporal shaping of the compressed pulse [27].

### **CBGs recorded in PTR glass**

As it was mentioned above, practical CBGs that can be installed in CPA ultrashort pulse laser systems became a reality when the technology of extremely high optical homogeneity PTR glass and the technology of extremely uniform large aperture hologram recording were demonstrated and made commercially available by the OptiGrate Corp ([www.optigrate.com](http://www.optigrate.com)). Currently, these technologies enable fabrication of CBGs for the spectral region from 0.8 to 2.5  $\mu\text{m}$  with low absorption and high laser-induced damage threshold that ensures compression of pulses with an energy exceeding 1 mJ and an average power exceeding 250 W. The aperture for commercially available CBGs is up to 10x10 mm<sup>2</sup> with a thickness up to 50 mm. The level of diffracted beam quality that has been achieved for such CBGs is currently  $M^2 < 1.4$ . A further extension of the aperture and thickness will be dependent upon achieving improvements in the PTR glass technology and large aperture hologram recording techniques.

The characteristics of the CBGs recorded in PTR glass are a strong function of the spectral range where they are intended to be used because of the dramatic difference in the feasible stretching factor SF (or spectral chirp rate, SCR) and scattering loss for different spectral regions. There are four main spectral regions and CBG product types where commercially available laser sources

may utilize CPA technology: type I CBGs for 0.8  $\mu\text{m}$  Ti: Sapphire lasers; type II for 1  $\mu\text{m}$  Yb and Nd doped fiber and solid state lasers, type III for 1.5  $\mu\text{m}$  lasers based on Er-doped fiber and solid state lasers, and type IV for 2  $\mu\text{m}$  novel laser sources that are currently under development.

### ***Type I CBGs for 0.8 $\mu\text{m}$ .***

The uses of CBGs in high power Ti: Sapphire laser systems have both positive and negative aspects. On one hand, the use of CBGs is very beneficial since they can handle high peak powers. However, the use of CBGs in this short wavelength spectral region is limited due to the limited spectral bandwidth and high scattering losses that affect the diffraction efficiency. Figure 8A shows the dependence of the maximum achievable diffraction efficiency and the minimum achievable scattering losses on the spectral bandwidth of CBGs operating at 800 nm. It is known [12] that an increase in the CBG spectral bandwidth requires a higher spatial refractive index modulation in the PTR glass. The maximum refractive index modulation in PTR glass of  $\sim 10^{-3}$  limits the achievable spectral width to about 20 nm for 800 nm operation. One can see that the diffraction efficiency decreases while the losses increase when the spectral width is increased. CBGs with a spectral bandwidth of 20 nm at 800 nm have diffraction efficiencies barely exceeding 50%. The main factor that restricts the diffraction efficiency of a CBG in this spectral range is the material losses caused by the light scattering in the bulk of the CBG material. As it was shown in the previous Section, a decrease in the spectral width of CBGs in this region requires a smaller refractive index modulation and, therefore, smaller scattering losses (Fig. 8A). CBGs designed for this spectral range can have stretching factors ranging from 15 to 300 ps/nm (Table 1). One can see that the maximum achievable stretching factor is inversely proportional to

the spectral bandwidth. From this table one can calculate the maximum dispersion that can be provided by CBGs. For gratings having a spectral bandwidth from 2 to 20 nm, the achievable stretching time is 500 ps.

### ***Type II CBGs for 1 $\mu\text{m}$***

In this spectral region a large variety of high power ultrafast lasers have been developed for industrial, medical and military applications. The achievable characteristics of CBGs in this spectral region meet the requirements of those lasers very well and this has led to a wide range in usage of CBGs in industrial and scientific ultra-short pulsed lasers at 1  $\mu\text{m}$ . The main advantage of this spectral region for the use of CBGs is the reduced light scattering as described in formula (7). Thus, gratings fabricated for the 1  $\mu\text{m}$  spectral range have significantly lower losses than for 0.8  $\mu\text{m}$ . Figure 8B shows the achievable diffraction efficiencies for this spectral range and the associated losses for chirped Bragg gratings with different spectral bandwidths. One can see that the diffraction efficiency is significantly enhanced compared to the gratings designed for the 800 nm laser wavelength. This lower level of material losses has allowed fabrication of gratings with spectral bandwidths up to 30 nm. Currently, CBGs at 1  $\mu\text{m}$  are commercially fabricated with stretching factors ranging from 7 to 500 ps/nm. Table 1 summarizes the achievable stretching factors for different spectral bandwidths.

### ***Type III CBGs for 1.5 $\mu\text{m}$***



Scattering losses in the 1.5  $\mu\text{m}$  spectral range impose an even smaller penalty on the CBG diffraction efficiency. One can see in Fig. 8C that the material losses at 1500 nm are reduced by nearly a factor of two compared to those losses at 1000 nm with the same bandwidth. This permits the fabrication of CBGs having spectral bandwidths up to 50 nm. The manufacturing of gratings with a larger bandwidth in this spectral region is limited by the refractive index modulation. Table 1 summarizes the stretching factors for gratings operating in the 1500 nm spectral region.

#### *Type IV CBGs for 2 $\mu\text{m}$*

The transparency window of PTR glass extends out to 2.9  $\mu\text{m}$  [17]. Volume Bragg gratings with a uniform grating period operating at this wavelength have been successfully manufactured in PTR glass, however, the extended thickness needed for CBGs in this wavelength region reduces the transparency window down to 2.7  $\mu\text{m}$ . Thus, this last type of VBG covers the region from 1800 to 2700 nm. In this region, the material losses due to scattering are smaller than 10% for all types of gratings. This is shown in Figure 8D which also shows the achievable diffraction efficiency as a function of spectral bandwidth. In this spectral region, the main limiting factor that restricts the spectral bandwidth is the refractive index modulation. However, despite this limitation, CBGs with spectral bandwidths up to 100 nm can be designed and fabricated for use in this spectral region.

Recently, the technology of PTR glass fabrication has been significantly advanced enabling the manufacture of CBGs with thicknesses exceeding 50 mm and apertures exceeding 10 mm. The

nearly diffraction-limited quality of the diffracted beam supports the usage of CBGs in high quality laser systems.

## **Conclusions**

Reflecting volume Bragg gratings recorded with the grating period gradually varying along the beam propagation direction provide effective stretching and recompression of short laser pulses. CBGs are monolithic devices that have three orders of magnitude smaller usage volumes compared to the conventional Treacy compressors. CBGs recorded in photo-thermo-refractive glass can be used in the spectral range from 0.8 to 2.5  $\mu\text{m}$  with diffraction efficiencies exceeding 90%, and provide pulse stretching up to 1 ns and compression down to 200 fs for laser pulses with energies and average powers exceeding 1 mJ and 250 W, respectively, while keeping the recompressed beam quality  $M^2 < 1.4$ .

**Acknowledgements.** The work was partially supported by Navy contracts NN00024- 09- C-4134 and N68335-12-C-0239 and HEL JTO contract W911NF-10-1-0441.

## **References**

1. D. Strickland and G. Mourou, "Compression of amplified chirped optical pulses," *Opt. Comm.* **56**, 219 (1985).
2. E. Treacy, "Optical pulse compression with diffraction gratings," *Quantum Electronics, IEEE Journal of*, **5**, no.9, 454-458 (1969).

3. O. Martinez. "3000 times grating compressor with positive group velocity dispersion: application to fiber compensation in 1.3-1.6  $\mu\text{m}$  region". IEEE J. Quant. Elect. 23 (1987) 59.
4. A. Boskovic, M. J. Guy, S. V. Chernikov, J. R. Taylor, and R. Kashyap, "All-fibre diode pumped, femtosecond chirped pulse amplification system," Electron. Lett. **31**, 877-879 (1995).
5. A. Galvanauskas, M. E. Fermann, D. Harter, K. Sugden, and I. Bennion, "All-fiber femtosecond pulse amplification circuit using chirped Bragg gratings," Appl. Phys. Lett. **66**, 1053-1055 (1995).
6. A. Galvanauskas, M. E. Fermann, "Optical pulse amplification using chirped Bragg gratings", US patent 5,499,134, March 12, 1996.
7. P. Hariharan. Optical Holography. Principles, techniques, and applications. *Chapter 7: "Practical recording materials," 95-124. Cambridge University Press, 1996. P. 95.*
8. V.A. Borgman, L.B. Glebov, N.V. Nikonorov, G.T. Petrovskii, V.V. Savvin, A.D. Tsvetkov. Photothermal refractive effect in silicate glasses. *Sov. Phys. Dokl.*, 34 (1989) 1011-1013.
9. L.B. Glebov, N.V. Nikonorov, E.I. Panysheva, G.T. Petrovskii, V.V. Savvin, I.V. Tunimanova, V.A. Tsekhomskii. Polychromatic glasses - a new material for recording volume phase holograms. *Sov. Phys. Dokl.*, 35 (1990) 878-880.
10. Oleg M. Efimov, Leonid B. Glebov, Larissa N. Glebova, Vadim I. Smirnov. Process for production of high efficiency volume diffractive elements in photo-thermo-refractive glass. United States Patent 6,586,141. July 1, 2003.
11. Vadim Smirnov, Emilie Flecher, Leonid Glebov, Kai-Hsiu Liao, and Almantas Galvanauskas. "Chirped bulk Bragg gratings in PTR glass for ultrashort pulse stretching and

- compression”. Proceedings of Solid State and Diode Lasers Technical Review. Los Angeles 2005, SS2-1.
12. Kai-Hsiu Liao, Ming-Yuan Cheng, Emilie Flecher, Vadim I. Smirnov, Leonid B. Glebov, and Almantas Galvanauskas. “Large-aperture chirped volume Bragg grating based fiber CPA system”. Opt. Express 15 (2007) 4876-4882.
  13. Leonid B. Glebov, Emilie Flecher, Vadim I. Smirnov, Almantas Galvanauskas, Kai-Hsiu Liao. Stretching and compression of laser pulses by means of high efficiency volume diffractive gratings with variable period in photo-thermo-refractive glass. US Patent 7,424,185 September 9, 2008.
  14. H. Kogelnik. “Coupled wave theory for thick hologram gratings”. The Bell System Technical Journal 48 (1969) 2909-2946.
  15. Igor V. Ciapurin, Leonid B. Glebov, Vadim I. Smirnov. “Modeling of phase volume diffractive gratings, part 1: transmitting sinusoidal uniform gratings”. Optical Engineering 45 (2006) 015802, 1-9.
  16. Igor V. Ciapurin, Derrek R. Drachenberg, Vadim I. Smirnov, George B. Venus, Leonid B. Glebov. “Modeling of phase volume diffractive gratings, part 2: reflecting sinusoidal uniform gratings, Bragg mirrors”. Opt. Engineering 51 (2012) 058001, 1-10.
  17. Sergiy Kaim, Sergiy Mokhov, Vadim Smirnov, Boris Ya. Zeldovich and Leonid B. Glebov. “Stretching and Compressing of Short Pulses by Chirped Volume Bragg Gratings: Analytic and Numerical Modeling”. Optical Engineering, to be published.
  18. L.B. Glebov. “Photochromic and photo-thermo-refractive (PTR) glasses”. *In Encyclopedia of Smart Materials, Volume 2. John Wiley & Sons, NY, 2002, 770-780*

19. T. Cardinal, O. M. Efimov, H. G. Francois-Saint-Cyr, L. B. Glebov, L. N. Glebova, and V. I. Smirnov, "Comparative study of photo-induced variations of x-ray diffraction and refractive index in photo-thermo-refractive glass," *J. Non-Cryst. Solids* 325, 275–281 (2003).
20. Leonid Glebov. "Fluorinated silicate glass for conventional and holographic optical elements". *Window and Dome Technologies and Materials X*, edited by Randal W. Tustison, *Proc. of SPIE Vol. 6545, 654507*, (2007).
21. Julien Lumeau, Larissa Glebova, and Leonid B. Glebov. "Near-IR absorption in high-purity photothermorefractive glass and holographic optical elements: measurement and application for high-energy lasers". *Appl. Opt.* 50 (2011) 5905-5911.
22. Derrek R. Drachenberg, Oleksiy Andrusyak, George Venus, Vadim Smirnov, Julien Lumeau, and Leonid B. Glebov. "Ultimate efficiency of spectral beam combining by volume Bragg gratings". *Appl. Opt.* 52 (2013) 7233-7242.
23. ISO Standard 11146, "Lasers and laser-related equipment – Test methods for laser beam widths, divergence angles and beam propagation ratios" (2005).
24. Anthony E. Siegman, "Defining, measuring, and optimizing laser beam quality", *Proc. SPIE* 1868, *Laser Resonators and Coherent Optics: Modeling, Technology, and Applications*, 2 (1993).
25. Sean Ross, William P. Latham. "Appropriate Measures and Consistent Standard for High Energy laser Beam Quality". *Journal of Directed Energy* 2 (2006) 22-58.
26. Kyungbum Kim, Laurent Vaissie, Robert Vaars, Andrew Stadler, Michael Cumbo. "Pulse stretcher and compressor including a multipass Bragg grating". US Patent 7,444,049. October 28, 2008.

27. Oleksiy Andrusyak, Lionel Canioni, Ion Cohanoshi, Martin Delaigue, Eugeniu Rotari, Vadim Smirnov, and Leonid Glebov. "Sectional Chirped Volume Bragg Grating Compressors for High-Power Chirped-Pulse Amplification". Proc. of SPIE 7578 (2010) Solid State Lasers XIX: Technology and Devices, ed. W.A. Clarkson, N. Hodgson, R.K. Shori. 75781A, 1-11.
28. Dylan Moses, Oleksiy Andrusyak, Marc SeGall, Julien Lumeau, Vadim Smirnov, Vasile Rotar, Leonid Glebov. "Stretching and compression of ultrashort pulses using chirped volume Bragg gratings in single- and multi-pass configurations". Advanced High Power Laser Review. 8th Annual Ultrashort Pulse Laser Workshop. Broomfield, CO. June 17, 2010.

### Figure captions

Fig. 1. Recording geometry for uniform gratings by interference of collimated beams (A) and for chirped gratings by interference of a convergent and a divergent beams (B). Arrows show the direction of the recording beam propagation. Z is the axis collinear to the grating vector.

Fig. 2. Schematics of beam diffraction by volume Bragg gratings. A – transmitting grating, B – uniform reflecting grating (Bragg mirror), C – chirped reflecting grating.  $\lambda_1 > \lambda_2 > \lambda_3$ . Spatial modulation is not in scale – the typical period for a Bragg mirror at 1  $\mu\text{m}$  is about 0.3  $\mu\text{m}$ .

Fig. 3. Modeled spectra of diffraction efficiency of lossless reflective gratings with different spectral chirp rates. Parameters of modeling: central wavelength  $\lambda_0 = 1550$  nm, spatial refractive index modulation  $\delta n = 700$  ppm, thickness  $T = 5$  mm. Spectral chirp rate  $d\lambda/dz$ , nm/cm: 1 – 0; 2 – 0.5; and 3 – 5.

Fig. 4. Dependence of time delay on wavelength (time delay dispersion) of a 50 mm thick CBG centered at 1555 nm with a spectral chirp rate of 3.2 nm/cm. Straight line – linear dispersion, squares – experimental data.

Fig. 5: The spectrum of the absolute diffraction efficiency of a CBG illuminated from the “red end” (1) and the spectra of the input (2) and diffracted beams: single pass (3) and double pass (4).

Fig. 6: Schematics of beam diffraction by multipass (A) and multi-sectional (B) CBGs. M – mirror, PM – phase mask.  $\lambda_1 > \lambda_2 > \lambda_3$ . Spatial modulation is not in scale – the typical period for a Bragg mirror at 1  $\mu\text{m}$  is about 0.3  $\mu\text{m}$ .

Fig. 7: The temporal profiles of a pulse stretched and recompressed by a double pass CBG without (A) and with a phase mask (B) placed before the retroreflector. This binary phase mask provides a phase shift  $k=\lambda/2$  for half of the beam.

Fig. 8. Diffraction efficiency and losses achieved in chirped Bragg gratings versus spectral bandwidth for different wavelengths.

Table 1. The parameters of chirped Bragg gratings used in the different spectral regions.

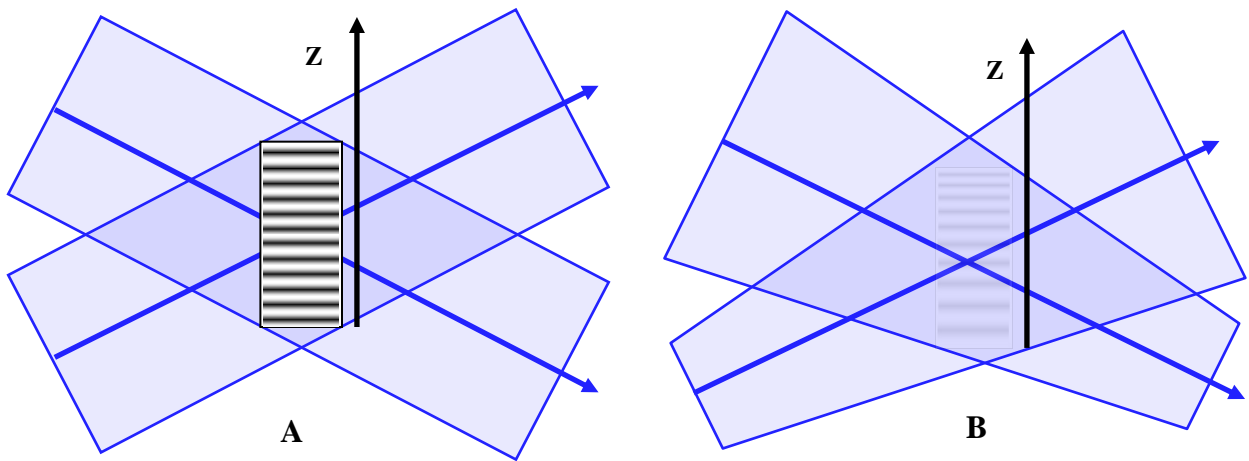


Fig. 1. Recording geometry for uniform gratings by interference of collimated beams (A) and for chirped gratings by interference of a convergent and a divergent beams (B). Arrows show the direction of the recording beam propagation.  $Z$  is the axis collinear to the grating vector.



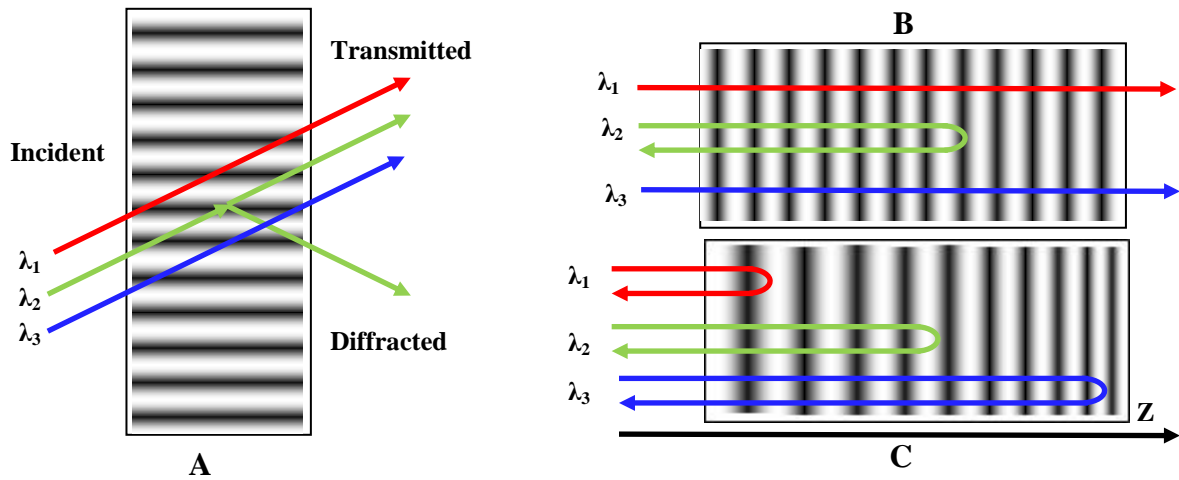


Fig. 2. Schematics of beam diffraction by volume Bragg gratings. A – transmitting grating, B – uniform reflecting grating (Bragg mirror), C – chirped reflecting grating.  $\lambda_1 > \lambda_2 > \lambda_3$ . The spatial modulation is not in scale – the typical period for a Bragg mirror at  $1 \mu\text{m}$  is about  $0.3 \mu\text{m}$ .

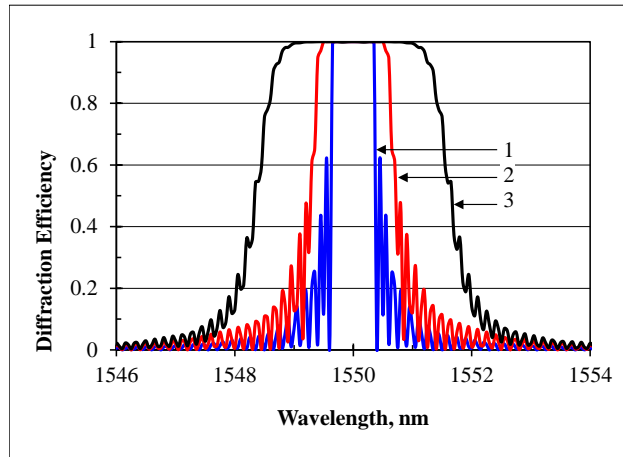


Fig. 3. Modeled spectra of the diffraction efficiency of lossless reflective gratings with different spectral chirp rates. The parameters of modeling: central wavelength  $\lambda_0=1550$  nm, spatial refractive index modulation  $\delta n=700$  ppm, thickness  $T=5$  mm. The spectral chirp rate  $d\lambda/dz$ , nm/cm: 1 – 0; 2 – 0.5; and 3 – 5.

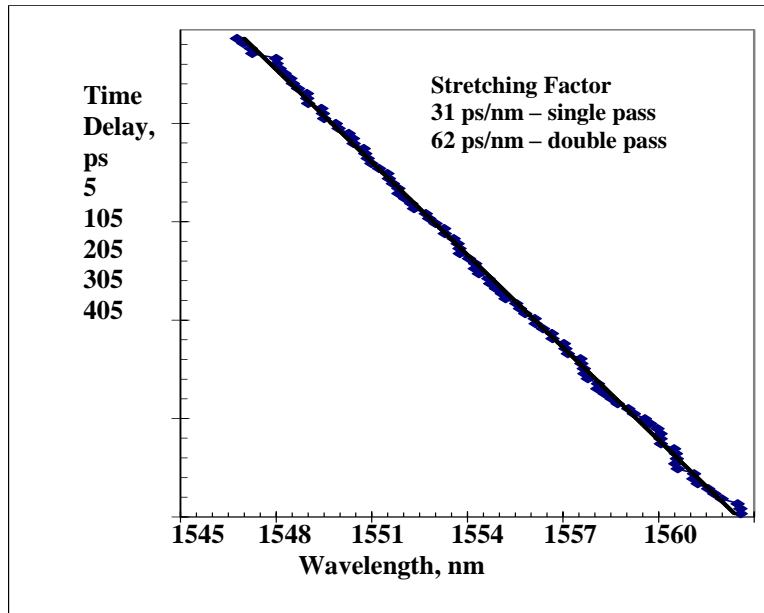


Fig. 4. The dependence of the time delay on wavelength (time delay dispersion) of a 50 mm thick CBG centered at 1555 nm having a spectral chirp rate of 3.2 nm/cm. Straight line – linear dispersion, squares – experimental data.

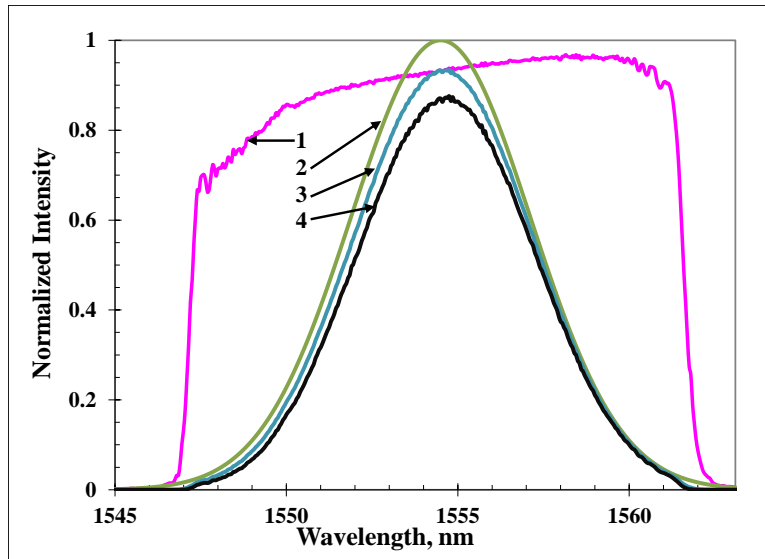


Fig. 5. The spectrum of the absolute diffraction efficiency of a CBG illuminated from the “red end” (1) and the spectra of the input (2) and diffracted beams: single pass (3) and double pass (4).

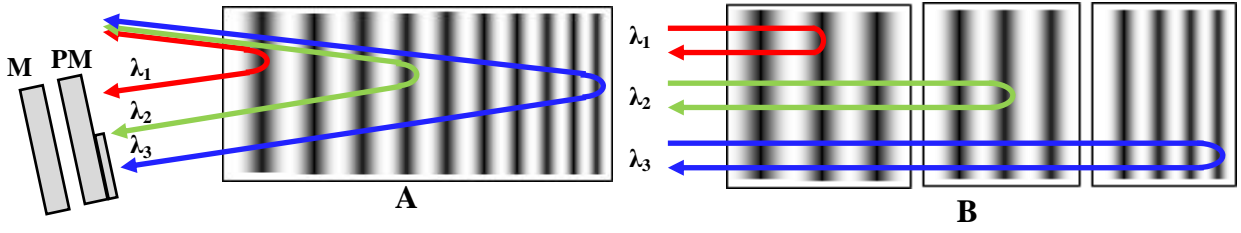


Fig. 6. Schematics of beam diffraction by multipass (A) and multi-sectional (B) CBGs. M – mirror, PM – phase mask.  $\lambda_1 > \lambda_2 > \lambda_3$ . The spatial modulation is not in scale – the typical period for a Bragg mirror at 1  $\mu\text{m}$  is about 0.3  $\mu\text{m}$ .

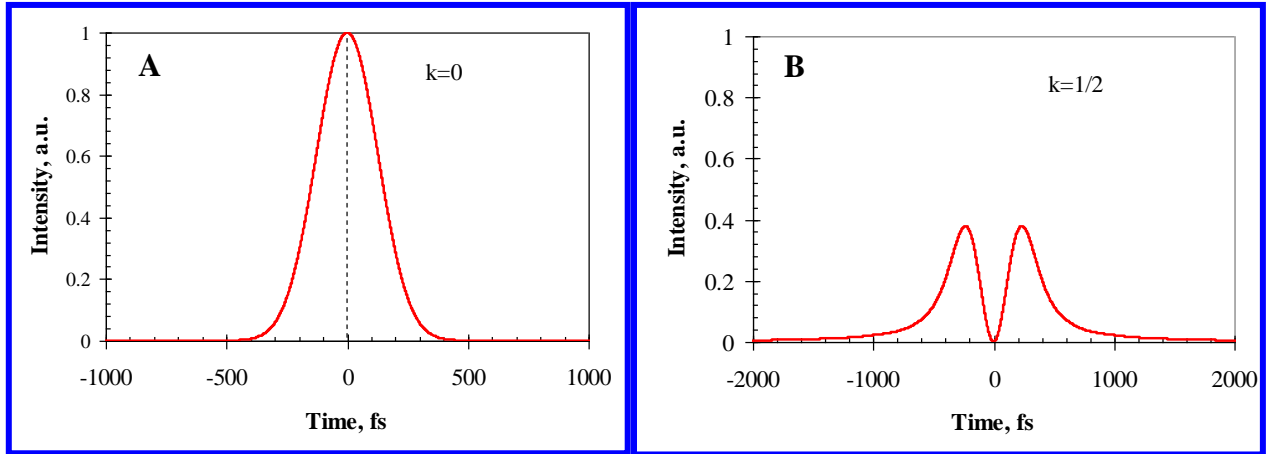


Fig. 7. The temporal profiles of a pulse stretched and recompressed by a double pass CBG without (A) and with a phase mask (B) placed before the retroreflector. This binary phase mask provides a phase shift  $k=\lambda/2$  for half of the beam.

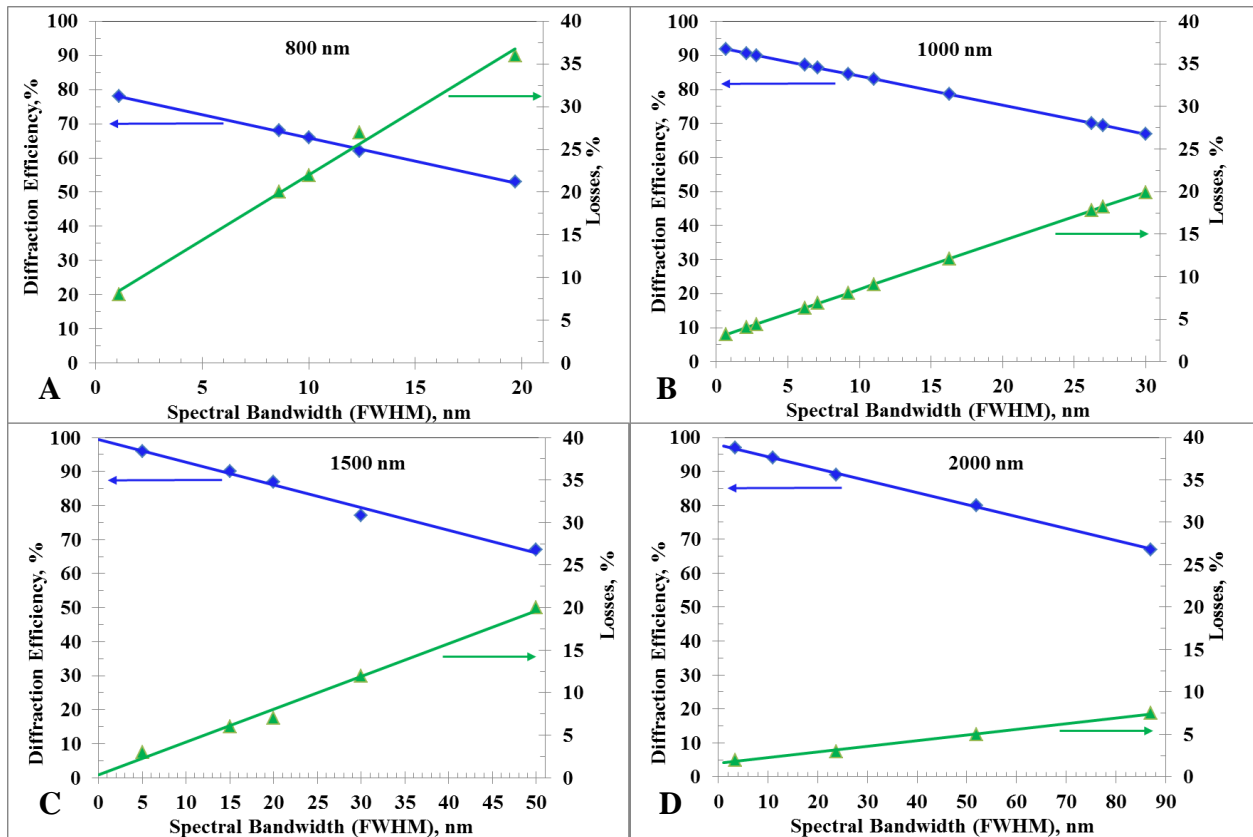


Fig. 8. Diffraction efficiency and losses achieved in chirped Bragg gratings versus the spectral bandwidth for different wavelengths.

Table 1. The parameters of chirped Bragg gratings used in the different spectral regions.

Wavelength, nm	Bandwidth, nm	Stretching Factor, ps/nm	
		Max	Min
800	1	300	15
	2	250	15
	5	100	15
	10	30	15
	20	15	15
1000	1	500	7
	2.5	170	7
	5	80	12
	10	30	12
	25	18	12
1500	2	150	20
	5	100	10
	10	50	10
	20	25	10
	50	10	10
2000	1	90	40
	5	90	20
	10	50	7
	50	10	7
	100	7	7



## **Biographies**

### **Leonid B. Glebov**

Leonid Glebov received his Ph.D. from the State Optical Institute, Leningrad, Russia (1976) and was affiliated with it up to 1995. Since 1995 Dr. Glebov has been at CREOL/UCF as a Research Professor. He is a founder and VP for R&D of OptiGrate Corp. He is a coauthor of a book, more than 300 papers in scientific journals and 10 patents. He is a Fellow of the ACerS, the OSA, the SPIE, and the NAI. He is a recipient of the Gabor award in holography. His main directions of research are optical properties of glasses, holographic optical elements, and lasers controlled by volume Bragg gratings.



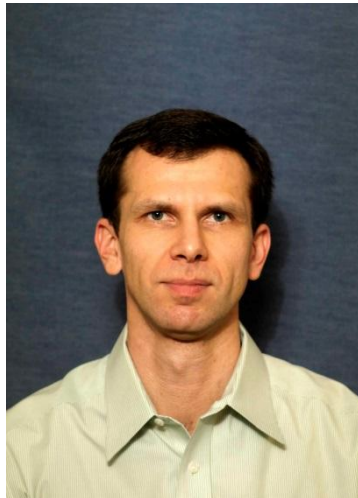
## **Vadim Smirnov**

In 1997 Vadim Smirnov joined CREOL and received MS. in Optics at the School of Optics/CREOL, University of Central Florida in 2000. He is a co-founder of OptiGrate and since 2003 holds the position at OptiGrate of the Director of Holography and Diffractive Optics. He was appointed to the position of Chief Technology Officer in 2010. He is the coauthor of more than 100 presentations and publications and three U.S. patents on high-efficiency diffractive elements in photo-thermo-refractive glass. His research activities include design and fabrication of volume diffractive gratings and holograms, nonlinear phenomena in optical glasses, and laser design.



## **Eugeniu Rotari**

Eugeniu Rotari received his Master of Science in Chemistry in 2002 from the State University of Moldova, Chisinau. In 2002 he joined the Photo-Processing Laboratory at CREOL/ The College of Optics and Photonics, University of Central Florida as a research scientist. Since 2005 he has been employed at Optigrate as an engineer and group leader focusing on optimization of volume Bragg grating recording in PTR glass, and automation of the testing and characterization of holographic optical elements. He participated in the development of recording and testing technologies for chirped Bragg gratings in PTR glass.



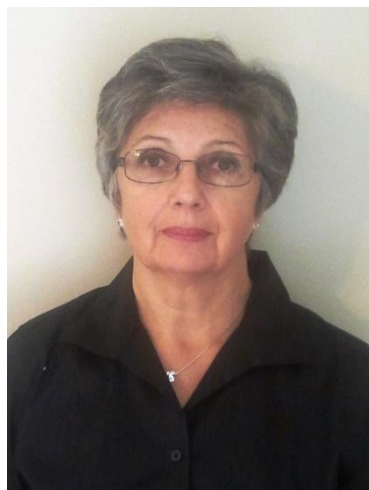
## **Ion Cohanoschi**

Ion Cohanoschi received his Ph. D. in Optics from the University of Central Florida, Orlando, USA, in 2006. Since 2007 he has been employed as an optical engineer at the OptiGrate Corporation. Previously, from 1995 to 2000 Ion Cohanoschi held the position of Physicist at the Nuclear Research Institute at Pitesti, Romania. Currently, Dr. Cohanoschi is a senior production engineer at OptiGrate and is responsible for the fabrication of Chirped Bragg Gratings (CBGs) and quality control of all VBGs. He has 17+ publications in refereed scientific journals and conference proceedings.



## **Larissa Glebova**

Larissa Glebova received her MS in Organic Chemistry from Tomsk Polytechnic Institute (Russia). She has been affiliated with UCF/CREOL since 1997 as a Research Scientist and with OptiGrate Corp. as the Director of Glass Technology since 1999 and Principal Glass Scientist since 2011. She is the co-author of 41 publications in scientific journals and holds two patents. The principal directions of Ms. Glebova's research include the technology of high purity homogeneous photosensitive glass, photo-thermo-induced structural transformations in glass, and the spectroscopy of glasses.



## **Oleg Smolski**

Oleg Smolski received the Ph.D. degree in Physics from Physico-Technical Institute in St Petersburg, Russia, in 1986. He held research positions in this institute, at the University of Connecticut, at CREOL at the University of Central Florida and at the University of North Carolina-Charlotte. His research activity covers semiconductor structures, epitaxial growth, optical glass melting, processing and packaging of laser diodes and optical glass components, and developing light-emitting devices with in-plane integrated and externally assembled diffractive optical elements. Beginning in 2012, he joined the management team of OptiGrate Corp. He is the co-author of over 50 scientific papers published in refereed journals and conference proceedings.



## **Julien Lumeau**

Julien Lumeau got M.S. and Ph.D. in Physics (major in Optics) from the Fresnel Institute, Marseille University, France respectively in 2001 and 2004. From 2005 until 2012, he worked at CREOL, University of Central Florida as a Faculty Research Scientist and was a consultant for the OptiGrate Corp. In 2013, he joined again the Fresnel Institute as a CNRS Senior Research Scientist. He is the authors of over 100 scientific communications including 40 peer-reviewed publications. The main directions of his research are photosensitive materials including their optical, nonlinear and crystallization properties and their use for new optical elements.



## **Christopher Lantigua**

Christopher Lantigua received his BS degree in electrical engineering from the University of Florida in Gainesville, Florida MS degree in Optics from University of Central Florida. He is now pursuing his PhD degree in Optics from the College of Optics and Photonics at the University of Central Florida in Orlando, Florida. His current research interests include holographic optical elements and nanophotonics.





## **Alexei Glebov**

Dr. Alexei Glebov is CEO and President of OptiGrate Corp. He received his Ph.D. and M.S. in Applied Physics from University of Gottingen, Germany, and University of St. Petersburg, Russia, respectively. He has started his industrial career at Bell Laboratories and worked for over a decade in engineering and management positions at Finisar, Fujitsu, and Lucent Technologies. He has 35 US patents and more than 50 peer-reviewed journal publications and book chapters. He is a frequent invited lecturer, editor of conference proceedings, conference and symposium chair, and executive organizing and program committee member at professional photonics meetings and trade shows.

